3rd URSI AT-AP-RASC, Gran Canaria, 29 May – 3 June 2022

Atmospheric propagation effects in the D-band with application to 5G-6G wireless communication systems

José Manuel Riera, Domingo Pimienta-del-Valle, Pedro Garcia-del-Pino
Universidad Politécnica de Madrid (UPM), Information Processing and Telecommunications Center (IPTC), Madrid, Spain, https://iptc.upm.es/

Abstract

The evolution of 5G wireless communications systems towards 5G-advanced and 6G technologies will need the use of millimeter-wave frequency bands above 60 GHz, including the D-band (110-170 GHz). Relevant propagation effects are present in this band because of the gases and hydrometeors in the troposphere, with the consequence that high attenuation can be produced even in relatively short links. These effects are studied in this paper on the basis of advanced meteorological measurements and physical models that could allow a reliable prediction of the attenuation caused in these frequencies. Some examples are provided for Madrid, Spain. The main conclusion of the paper is that the expected variability of the atmospheric attenuation is much higher than at lower frequency bands and must be taken into account in new radio planning procedures. However, D-band links with distances up to 1-2 km could be considered as feasible and can provide huge transmission capabilities in future wireless networks.

1. Introduction

The current 5G standard [1] includes the use of mm-wave (millimeter wave) frequencies up to 52.6 GHz in the Radio Access Network. Backhaul/fronthaul connections with data rates in the order of Gbit/s are needed in this context. When fiber optic is not available, mm-wave fixed links can be used instead. Currently the E-band (60-90 GHz) is a good alternative to deploy these fixed links. In a near future, 5G-advanced technologies defined in the futures Releases 17 and 18 of 3GPP will probably use higher frequencies in the access part of the network, sharing these spectral resources with backhaul/fronthaul links or moving these to higher frequencies above 100 GHz. Looking further into the future evolution towards 6G, it seems very likely that frequencies within the mm-wave band and above 100 GHz will be needed, at least for the part of the network based on fixed links.

In this context, a research has been carried out within the H2020 Ariadne project [2] in order to assess the influence of the atmosphere on the propagation of D-band (110-170 GHz) radio waves. From the literature search, only a short number of documents have reported rain attenuation measurements above 100 GHz, as for example [3]-[4] among others. Propagation campaigns intended to provide complete sets of data with all possible meteorological conditions need to be carried out for several years. Until data of these kinds are available, some estimations can be obtained with the use of meteorological data and physical models, based on the physical interactions of the radio waves with atmospheric gases and particles, and thus expected to provide reliable attenuation predictions.

The attenuation caused by the presence of the tropospheric gases and rain are the main propagation effects caused by the atmosphere in the D-band. Gas attenuation is analyzed in Section 2 using as input data Synoptic Data gathered by the Meteorological Offices and the physical model provided in ITU-R Rec. P.676-12 [5], which allows calculating the attenuation by atmospheric gases. Section 3 is dedicated to assess rain attenuation by using physical models of scattering of electromagnetic waves in particles with sizes comparable to their wavelength. The application of these models requires as input data the drop size distributions (DSD) of the rain particles, which are not usually available for most sites. This research makes use of an extensive database available at Universidad Politécnica de Madrid (UPM) in Madrid, Spain with twelve years (2008-2019) of DSD data [6], which allows estimating rain attenuation with high accuracy and detail. The main conclusions are drawn in Section 4.

2. Gas attenuation

Attenuation due to atmospheric gases can be estimated using the MPM model (Millimeter-Wave Propagation Model), adopted by ITU-R in Rec. P. 676-12 [5], and valid up to 1000 GHz, which calculates the specific attenuation, γ_g, (dB/km), as the sum of the contributions of the oxygen and water vapor resonance lines and a water vapor continuum component. The latter is empirically defined, and its effect strongly contributes to attenuation in frequencies located apart from absorption line peaks.

The value of γ_g depends on the frequency, temperature, atmospheric pressure, and water vapor density. Figure 1 shows the specific attenuation using the ITU-R model, calculated from 70 to 200 GHz at 1 GHz intervals, for a standard atmosphere: temperature of 15°C, pressure of 1013 hPa, and water vapor density of 7.5 g/m^3.

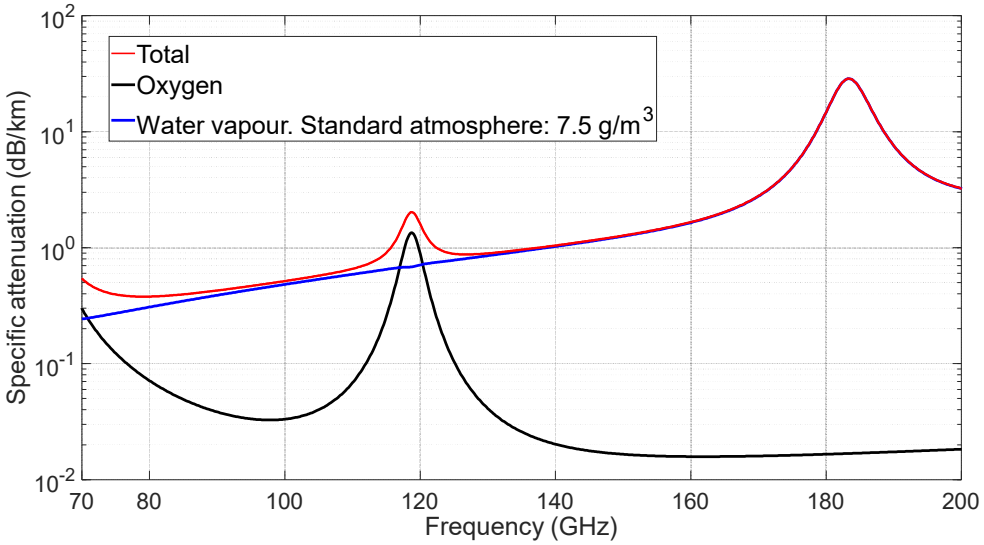

Figure 1. ITU-R model specific attenuation by oxygen, water vapor and total atmospheric gases for a standard atmosphere with temperature of 15 °C, pressure of 1013 hPa, and water vapor density of 7.5 g/m^3.

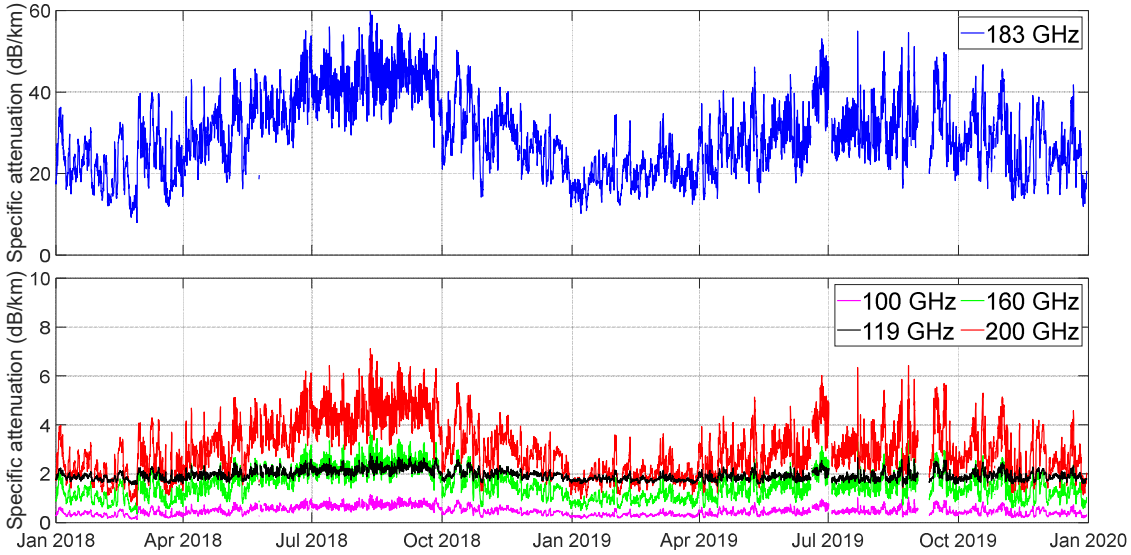

Figure 2. Estimated specific attenuation by gases in Madrid for 2018-2019 and frequencies 100-200 GHz

In Figure 1, the oxygen absorption line at 118.7 GHz is clearly identifiable. Apart from this peak, water vapor is the dominant effect, with a strong peak at 183.3. GHz.

Figure 2 presents an estimation of the specific attenuation expected in Madrid, Spain at several frequencies, using as input data two years (2018-19) of SYNOP (surface synoptic observations) reports, whose WMO format is FM-12 [7], used for reporting weather observations made by manned and automated weather stations. From [5] it can be obtained that oxygen attenuation is relatively stable, with only a small variation with temperature. However, water vapor attenuation depends on the water vapor content and therefore reflects its large variability. This large variability, in relative terms, is observed in Figure 2 for all frequencies, but its relevance is smaller in absolute terms for lower frequencies, with lower attenuation, and higher for the higher ones, peaking at 183 GHz, represented in a separate plot with a different scale.

Below 100 GHz, radio planning uses a single reference value for gas attenuation, calculated for the specific climatic conditions. The behavior of attenuation is similar to that shown in Figure 2 for 110 GHz. This approach is no longer valid for higher frequencies. Figure 3 represents the Complementary Cumulative Distribution Function (CCDF) of gas attenuation in Madrid at 160 GHz, calculated from the time series shown in Figure 2 for this frequency. The specific attenuation varies within a range (0.6-3.1 dB/km) much wider –in absolute terms– than that obtained at lower frequencies. This variability should be taken into account for radio planning at such high frequencies (and above), in addition to the influence of the climatic conditions.

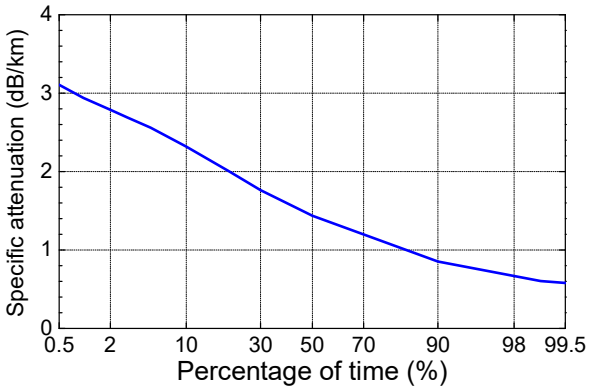

Figure 3. CCDF of specific attenuation by gases (estimated) in Madrid at 160 GHz

3. Rain attenuation

Rain attenuation semi-empirical models, as the one recommended by ITU-R [8] use as input data the rainfall rate with integration time of 1 minute. Rainfall rate is a convenient parameter since it can be available for multiple sites; however, the validity of this approach must be checked for higher frequencies. Based on a physical approach, if discrete experimental DSD are available, the specific rain attenuation γ_R (dB/km) can be estimated with (1) and appropriate unit conversions.

$$\gamma_R = \frac{10}{\ln 10} \sum_{i=1}^{M} \sigma_{ext}(D_i) N(D_i) dD_i \qquad (1)$$

where $N(D_i)$ ($m^{-3}mm^{-1}$) is defined as the number of particles per volume (m^3) and diameter D (mm) units for the class with central diameter D_i and is a way to quantify the Drop Size Distributions (DSD); $\sigma_{ext}(D_i)$ (mm^2) is the extinction cross section for the D_i diameter, dD_i is the class width and M is the total number of classes.

In this research, the DSD gathered in Madrid in 2008-2019 have been used to calculate rain attenuation. The data have been registered with a Thies Laser disdrometer [9], which measures the size and terminal velocity of each drop with the technique illustrated in Figure 4.

Figure 4. Conceptual scheme of the measurement of size and terminal velocity of drops with a laser disdrometer. Drop size and velocity are derived from the obstruction of the infrared laser beam (green area).

Only liquid precipitation is considered in this study, discarding hail and snow. For each minute of rain, the DSD is calculated from the raw spectra of drop sizes and velocities provided by this instrument. Then, rain attenuation is calculated using three different sets of extinction cross sections, whose description can be found in much more detail in [10]. One set is analytically obtained using the Mie theory of scattering in spherical drops. The two others consider a model of non-spherical raindrops and apply electromagnetic simulations to calculate the extinction cross sections for horizontal (H) and vertical (V) polarization. The comparison of the three sets for 150 GHz is shown in Figure 5.

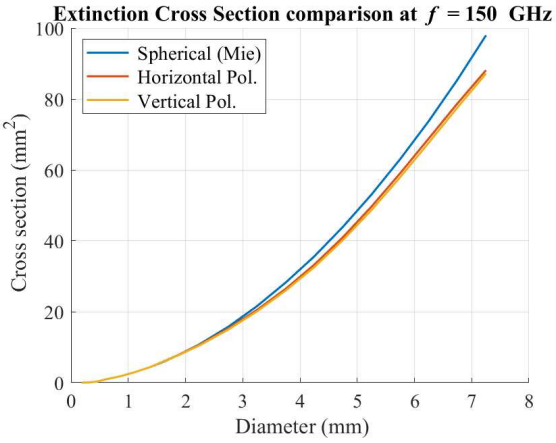

Figure 5. Extinction cross-sections for spherical drops and non-spherical drops (H and V polarization).

As a difference with lower frequencies, the two polarizations (H and V) have very similar extinction cross sections. For the highest drop diameters, much larger than the signal wavelength, the electromagnetic simulations predict a smaller extinction cross-section for non-spherical than for spherical drops.

Figure 6 shows the specific attenuation derived at 150 GHz versus rainfall rate and for each minute of rain considering non-spherical drops and horizontal polarization.

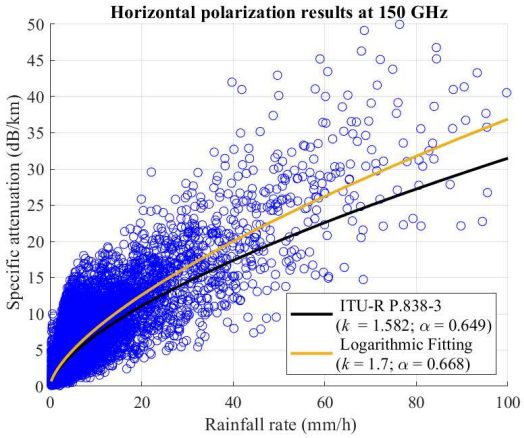

Figure 6. Specific rain attenuation versus rainfall rate, non-spherical drops, 150 GHz (2008-19).

Each blue circle in Figure 6 corresponds to one minute of rain in the period 2008-19. Both the rainfall rate and the attenuation have been calculated from the DSD, the latter using (1) and the set of extinction cross-sections obtained for 150 GHz and horizontal polarization. Two curves are also plotted in Figure 6, one (mustard) obtained by logarithmic fitting of the one-minute points and another (black) using the ITU-R Rec. P.838-3 predictions [8]. In both curves the following relation is assumed:

$$\gamma_R = kR^{\alpha} \qquad (2)$$

where R(mm/h) is the rainfall rate and k and α are parameters dependent on frequency and polarization. Figure 6 shows that this law and the ITU-R recommended parameters represents well the central values of attenuation versus rain rate, but that a large variation of attenuation around these central values, in comparison with lower frequencies, is a key characteristic of rain attenuation in these band. This variability has been modeled in [10].

Rain attenuation for a 0.1-km link working at 150 GHz with horizontal polarization has been calculated by multiplying the distance by the specific attenuation, since rainfall rate is constant within this short distance. The CCDFs of attenuation for each of the twelve years under study and for the full period are shown in Figure 7. Attenuation exceeded 0.001% of the period ranges between 2-6 dB, which makes a link of these characteristics feasible with very high availability. Extrapolating these results, it can be concluded that D-band links can provide very high data rate transmissions with high availability (above 99.99%) for distances of several hundred meters or up to 1-2 km, depending on the local rain regime and the required availability.

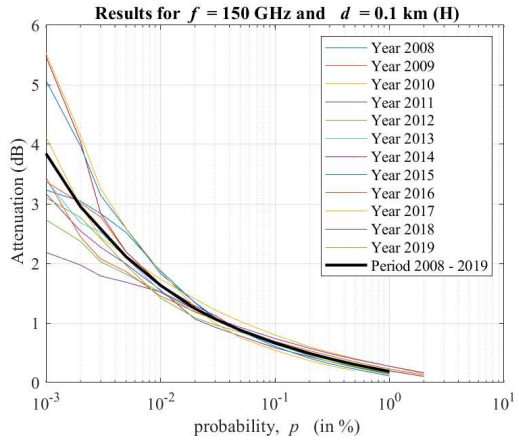

Figure 7. CCDF of attenuation for a 0.1-km link in Madrid at 150 GHz with horizontal polarization.

4. Conclusions

Gas and rain attenuation have a different behavior, hence different impact, in the D-band than at lower frequency bands. For both propagation effects, their variability must be accounted for in new ways: in the first case, a single reference value of gas attenuation would not suffice for planning purposes; in the case of rain attenuation, its variability around central values is much higher than at lower frequencies. This is due to DSD spread and should be considered in future models.

Notwithstanding these considerations, D-band links with distances up to 1-2 km can be feasible and can provide huge transmission capabilities with high availability in future 5G-6G wireless networks.

6. Acknowledgements

This work was supported in part by the Ministry of Science, Innovation and Universities of Spain through the RTI2018-098189-B-I00 project and by Horizon 2020, European Union Framework Program for Research and Innovation, under Grant Agreement no. 871464 (ARIADNE).

References

[1] J.T.J. Pentinnen “5G Second Phase Explained”, Wiley, 2021.
[2] https://www.ict-ariadne.eu/
[3] A. Hirata et al., "Effect of Rain Attenuation for a 10-Gb/s 120-GHz-Band Millimeter-Wave Wireless Link," *IEEE Transactions on Microwave Theory and Techniques*, vol. 57, no. 2, pp. 3099-4006, December 2009
[4] S. Ishii, S. Sayama, and T. Kamei, "Measurement of Rain Attenuation in Terahertz Wave Range," *Wireless Engineering and Technology*, vol. 2, pp. 119-124, July 2011.
[5] ITU-R Rec. P.676-12, “Attenuation by atmospheric gases”, ITU Radiocommunication Bureau, Geneva, Switzerland, Sep. 2019
[6] J. M. Riera, A. Benarroch, P. Garcia-del-Pino and S. Pérez-Peña, "Preprocessing and Assessment of Rain Drop Size Distributions Measured with a K-Band Doppler Radar and an Optical Disdrometer," in *IEEE Transactions on Instrumentation and Measurement*, vol. 70, pp. 1-8, 2021
[7] World Meteorological Organization, WMO-No. 306, “Manual on Codes”, Geneva, Switzerland, 2011 [9] ITU-R Rec. P.838-3
[8] ITU-R Rec. P.838-3, "Specific attenuation model for rain for use in prediction methods," ITU Radiocommunication Bureau, Geneva, Switzerland, 2005.
[9] ADOLF THIES GmbH & Co. KG, "Laser Precipitation Monitor, Instruction for Use," v2.0x STD 2005.
[10] D. Pimienta-del-Valle, J.M. Riera, S. Pérez-Peña, P. Garcia-del-Pino and A. Benarroch, “Characterization of Rain Attenuation in 80-200 GHz Radio Links Considering Non-Spherical Raindrops”, *Proc. Of EuCAP,* March 27th to April 1st 2022, Madrid, Spain.